

# Manuscript Draft: Aim3 Leaf Traits

Bolívar Aponte Rolón      Mareli Sánchez Juliá      A. Elizabeth Arnold  
Sunshine A. Van Bael

2023-12-07

## 1 Abstract

## 2 Introduction

## 3 Methods

### 3.1 Field

Growth and host plant inoculation seven tropical tree species was conducted at the greenhouses in the Gamboa Research Station, Smithsonian Tropical Research institute, Republic of Panama. The species, *Theobroma cacao*, *Dypterix* sp., *Lacmellea panamensis*, *Apeiba membranacea*, *Heisteria concinna*, *Chrysophyllum caimito*, and *Cordia alliodora* were chosen due to their variance in leaf traits (J.Wright unpublished data) and the availability of seeds in January- April 2019. Seeds of tree species were collected from the forest floor and grown in the greenhouse. Seedlings were kept in a chamber made out of PVC and clear plastic to prevent inoculation from spore fall inside the greenhouse. NEEDS

16 INFORMATION ON THE SOIL MIXTURE AND AUTOCLAVING PROTOCOL. Seedlings reached  
17 a minimum of 4 true leaves before endophyte inoculation. Then 10 individual plants of each species  
18 were exposed to 10 nights of spore fall to achieve a high endophyte load (E+) and 10 homologous plants  
19 were kept inside the greenhouse plastic chamber to maintain a low endophyte load (E-) (Fig. ? MAKE A  
20 DIRAGRAM?). Plants exposed to spore fall were placed near (~10 m) the forest edge at dusk (~18:00  
21 hours) and returned to the greenhouse at dawn (~07:00 hours) (Bittleston et al. 2011).

### 22 3.1.1 Leaf trait measurements

23 Three mature leaves were haphazardly collected from each of the individual plants in each treatment  
24 (E+, E-) within 7-10 days after inoculation treatment. Anthocyanin (ACI) content and leaf thickness  
25 (LT) were measured while the leaf was still attached to the plant. We measured anthocyanin content with  
26 ACM-200plus (Opti-Sciences Inc. Hudson, New Hampshire, U.S.A.) on three haphazardly selected lo-  
27 cations (working from the petiole out to the leaf tip) on the leaf surface of three haphazardly selected  
28 leaves for a total of nine measurements per plant (Tellez et al., 2022). The ACM-200 calculates an  
29 anthocyanin content index (ACI) value from the ratio of % transmittance at 931 nm/% transmittance  
30 at 525 nm (**opti-sciencesinc?**) . On compound leaves (i.e., *Dypterix* sp.) we measured at three differ-  
31 ent leaflets. Leaf thickness ( $\mu\text{m}$ ) was measured with a Mitutoyo 7327 Micrometer Gauge (Mitutoyo,  
32 Takatsu-ku, Kawasaki, Japan) in sthe same manner as the anthocyanin measurements, taking care to  
33 avoid major and secondary veins. After anthocyanin and leaf thickness measurements were completed,  
34 we removed the leaves from their stems, placed them inside a plastic bag (i.e. Ziploc ), place in an ice  
35 chest and moved them to the lab for further measurements. Leaf punch strength (LPS) was measured

with an Imada DST-11a digital force gauge (Imada Inc., Northbrook, IL, United States) by conducting punch-and-die tests with a sharp-edged cylindrical steel punch (2.0 mm diameter) and a steel die with a sharp-edged aperture of small clearance (0.05 mm). The leaf punch measurements were taken by puncturing the leaf lamina at the base, mid-leaf and tip on both sides of the mid-vein, avoiding minor leaf veins when possible (Tellez et al., 2022). Once leaf toughness was measured, we used a 7 mm diameter punch hole to puncture disks for leaf mass per area (LMA) measurements. We collected one three disks per leaf (see Supplementary material for details). The disk punches dried at 60 °C for 48-72 hours. before being weighed.

### **3.1.2 Leaf tissue preparation for molecular work**

The selected leaves were also used to profile endophyte community composition, abundance, and richness via amplicon sequencing (Illumina MiSeq). The leaf tissue remaining after the leaf trait measurements had the main vein and margins excised so that only the lamina remained. The lamina was haphazardly cut into 2 x 2 mm segments, enough to obtain a total of 16, and surface sterilized by sequential rinsing in 95% ethanol (10 s), 0.5 NaOCl (2 mins) and 70% ethanol (2 mins), as per (Arnold et al., 2003; Higgins et al., 2014; Tellez et al., 2022). After, leaves were air-dried briefly under sterile conditions. Sixteen leaf segments per leaf, a total of forty-eight leaf segments per plant, were plated in 2% malt extract agar (MEA), sealed with Parafilm M (Bemis Company Inc., U.S.A.) and incubated at room temperature. The cultured leaf segments were used to estimate endophyte colonization of E+ and E- leaves. The presence or absence of endophytic fungi in the leaf cuttings was assessed 7 days after plating. The remaining sterilized leaf lamina was preserved in sterile 15 mL tubes with ~ 10 mL

CTAB solution (1 M Tris-HCl pH 8, 5 M NaCl, 0.5 M EDTA, and 20 g CTAB). Leaf tissue in CTAB solution was used for amplicon sequencing (described in detail below). All leaf tissue handling was performed in a biosafety cabinet with all surfaces sterilized by exposure to UV light for 30 minutes and cleaned sequentially in between samples with 95% ethanol, 0.5% NaOCl and 70% ethanol to prevent cross contamination.

### 3.2 Amplicon sequencing

Leaf tissue in CTAB solution was stored for 2 months at room temperature prior to being placed at -80 C for 3 months before extracting DNA. In preparation for DNA extraction, we decontaminated all instruments, materials, and surfaces with DNAway (Molecular BioProducts Inc., San Diego, CA, United States), 95% Ethanol, 0.5 % NaOCl, and 70 % Ethanol, and subsequently treated with UV light for 30 minutes in biosafety cabinet. We then transferred 0.2 – 0.3 g of leaf tissue into duplicate sterile 2mL tubes, resulting in 2 subsamples. Total genomic DNA from subsamples was extracted as described in U'Ren & Arnold (2017). In brief, we added two sterile 3.2 mm stainless steel beads to each tube and proceeded to lyophilize samples for 72 hours to fully remove CTAB content from tissue. After this period, we submerged the sample tubes in liquid nitrogen for 30s and proceeded to homogenize samples to a fine powder for 45 s in FastPrep-24 Tissue and Cell Homogenizer (MP Biomedicals, Solon, OH, USA). Afterwards, we repeated the decontamination procedure described before and used QIAGEN DNeasy 96 PowerPlant Pro-HTP Kit (U'Ren & Arnold, 2017) (QIAGEN, Valencia, CA, USA). After all genomic DNA was extracted, we pooled the subsamples for each individual sample before amplification. We used sterile equipment and pipettes with aerosol-resistant tips with filters in all steps before

76 amplification. We followed a two-step amplification approach previously described by Sarmiento et  
77 al. (2017) and U'Ren & Arnold (2017). We used primers for the fungal ITSrDNA region, ITS1f (5'-  
78 CTTGGTCATTTAGAGGAAGTAA-3') and ITS4 (5'-TCCTCCGCTTATTGATATGC-3') with modi-  
79 fied universal consensus sequences CS1 and CS2 and 0–5 bp for phase-shifting. Every sample was  
80 amplified in two parallel reactions containing 1–2 µL of DNA template (U'Ren & Arnold, 2017; see  
81 also Tellez et al., 2022). We visualized PCR (PCR1) reactions with SYBR Green 1 (Invitrogen, Carls-  
82 bad, CA, USA) on 2% agarose gel (Oita et al., 2021). Based on the electrophoresis band intensity, we  
83 combined parallel PCR1 reactions and diluted 5 µL of amplicon product with molecular grade water  
84 to standardize to a concentration of 1:15 (Sarmiento et al., 2017 for details; Tellez et al., 2022). We in-  
85 cluded DNA extraction blanks and PCR1 negatives in this step. We used a separate set of sterile pipettes,  
86 tips, and equipment to reduce contamination. We used a designated PCR area to restrict contact with  
87 pre-PCR materials (Oita et al., 2021).

88 We used 1 µL of PCR1 product from samples and negative control for a second PCR (PCR2) with  
89 barcode adapters (IBEST Genomics Resource Core, Moscow, ID, USA). Each PCR2 reaction (total  
90 15 µL) contained 1X Phusion Flash High Fidelity PCR Master Mix, 0.075 µM of barcoded primers  
91 (forward and reverse pooled at a concentration of 2 µM) and 0.24mg/mL of BSA following Sarmiento  
92 (2017) and U'Ren & Arnold (2017). Before final pooling for sequencing, we purified the amplicons  
93 using Agencourt AMPure XP Beads (Beckman Coulter Inc, Brea, CA USA) to a ratio of 1:1 following  
94 the manufacturer's instructions. The products were evaluated with Bio Analyzer 2100 (Agilent Tech-  
95 nologies, Santa Clara, CA, USA) (Tellez et al., 2022). We quantified the samples through University  
96 of Arizona Genetics Core, and subsequently diluted them to the same concentration to prevent over

97 representation of samples with higher concentration, see (CITATION). Amplicons were normalized  
98 to 1 ng/μL, then pooled 2 μL of each for sequencing. No contamination was detected visually or by  
99 fluorometric analysis. To provide robust controls we combined 5 μL of each PCR1 negative and the  
100 DNA extraction blanks and sequenced them as samples. Ultimately, we combined samples into a single  
101 tube with 20 ng/μL of amplified DNA with barcoded adapters for sequencing on the Illumina MiSeq  
102 platform with Reagent Kit v3 (2 × 300 bp) following protocols from the IBEST Genomics Resource  
103 Core at the University of Idaho, USA. Again, we included the DNA extraction blanks and two PCR1  
104 negatives and sequenced with samples. Sequencing yielded 3,778,081 total ITS1 reads.

### 105 **3.2.1 Mock Communities**

106 We processed and sequenced 12 mock communities following the methods described above. This al-  
107 lowed us to assess the quality of our NGS data set. We used two mock communities that consisted of  
108 PCR product from DNA extractions of 32 phylogenetically distinct fungi, representing lineages that  
109 are typically observed as endophytes: Ascomycota, Basidiomycota, Zygomycota and Chytridiomycota  
110 (Oita et al., 2021; see Daru et al., 2019 for details). In brief, we used six mock communities with  
111 equimolar concentrations of DNA from all 32 fungal taxa and another six mock communities with  
112 tiered concentrations of DNA from the same fungal taxa (Daru et al., 2019). Each mock community  
113 was sequenced five times (i.e., five replicates) (Oita et al., 2021). The read abundance from the equimo-  
114 lar and tiered communities was positively associated with the expected read number (with replicates as  
115 a random factor:  $R^2_{Adj} = 0.87$ ,  $P = XXXX$ , see Supplementary Material). Using mock communities  
116 allowed us to evaluate the sequencing effectiveness in communities with known composition and struc-

ture (Bowman & Arnold, 2021). Henceforth, we used read abundance as a relevant proxy for biological OTU abundance (U'Ren et al., 2019).

### 3.2.2 Bioinformatic analyses

We used VSEARCH (v2.14.1) for *de novo* chimera detection, dereplication and sequence alignment. VSEARCH is an open-source alternative to USEARCH that uses an optimal global aligner (full dynamic programming Needleman-Wunsch), resulting in more accurate alignments and sensitivity (Rognes et al., 2016). For mock communities and experimental samples, we used forward reads (ITS1) for downstream bioinformatics analyses due to their high quality, rather than reverse reads (ITS4). Following Sarmiento et al. (2017), we concatenated all reads in a single file and used FastQC reports to assess Phred scores above 30 and determine the adequate length of truncation. We processed 892,713 of sequence reads from mock communities and 3,778,081 from experimental samples. We truncated mock community and experimental sample reads to a length of 250 bp with command `fast_truncLen` and filtered them at a maximum expected error of 1.0 with command `fast_maxee`. We then clustered unique sequence zero radius OTUs (that is, zOTUs; analogous to amplicon sequence variants (Callahan et al., 2016)), by using commands `derep_fulllength` and `minseqlength` set at 2. Sequentially we denoised and removed chimeras from read sequences with commands `cluster_unoise`, and `uchime3_denovo`, respectively (see Supplementary YYY for details). Finally, we clustered zOTUs at a 95% sequence similarity with command `usearch_global` and option `id` set at 0.95. After which, 3,035,960 sequence reads from experimental samples remained.

Taxonomy was assigned with the Tree-Based Alignment Selector Toolkit [v2.2; Carbone et al. (2019)]

by placing unknowns within the Pezizomycotina v2 reference tree (Carbone et al., 2017). ITS sequences were blasted against the UNITE database by the ribosomal database project (RDP) classifier. A total of 2147 OTUs hits were obtained and are composed of 68.6% Ascomycota, 26.8% Basidiomycota, <0.05% Chytridiomycota, <0.05% Glomeromycota, <0.05% Mortierellomycota, <0.05% Rozellomycota, 0.05% Kickxellomycota, and 4.2 % BLAST hit misses. Only OTUs representing Ascomycota were used for downstream statistical analyses since foliar endophyte communities in tropical trees are dominated by Ascomycota (Arnold & Lutzoni, 2007).

For each OTU identified, we removed laboratory contaminants from experimental samples by subtracting the average read count found in control samples from the DNA extraction and PCR steps. Our analysis of mock communities allowed use to identify and remove false OTUs from experimental samples, those with fewer than 10 reads, and remove 0.1% of the read relative abundance across all samples (Oita et al., 2021). Removed reads represent the frequency of reads classified as contamination in the mock communities relative to the expected read count. Three experimental samples from *Theobroma cacao* ( $n=2$ ) and *Apeiba membranacea* ( $n=1$ ) were removed from all analyses due to incomplete entries. After pruning taxa with zero reads from experimental samples, we identified 260 OTUs found exclusively in control ( $E-$ ) plants ( $n=78$ ) and deemed them as artifacts resulting from the greenhouse conditions. Consequently, these were consistently eliminated from treatment ( $E+$ ) plants across all species. We converted reads for each fungal OTU to proportions of total sequence abundance per sample to reduce differences in sampling effort, following previous studies (Weiss et al. (2017); McMurdie & Holmes (2014) ). We then removed singletons and obtained an average of 2,464,558 sequence reads in 529 Ascomycota OTUs across 156 experimental samples of 7 tree species. All analyses post taxonomic as-



158 signment were performed in R [v. 4.3.2; R Core Team (2023)] using the phyloseq package (McMurdie  
159 & Holmes, 2013) and custom scripts (see Supplementary Material).

### 160 **3.2.3 Ant-endophyte interaction assays**

161 A fresh fourth leaf was used in ant assays. To assess leaf-cutter ant damage, we introduced one detached  
162 leaf per plant per treatment to an actively foraging leaf-cutter ant colony for a two-hour assay. We  
163 presented leaf-cutter ant colonies with a choice of an E+ or an E- leaf on one disposable plastic plate  
164 next to an active nest trail. Carefully, we collected and placed debris from the trail leading up to the plate  
165 to lure ants into the plate. We initiated the ant assay as soon as one ant entered the plate and explored  
166 the leaf contents (for ~ 10-20 seconds). Every five minutes we took a digital photo of the choice arena  
167 until about 75% of the leaf content of one of the leaves was consumed. We used the digital photo at  
168 time zero and at the end of trial to quantify the leaf area removed using ImageJ [v1.52r; Schneider et  
169 al. (2012)]. Ant recruitment was estimated by counting individuals in the choice arena throughout trial  
170 event.

### 171 **3.2.4 Pathogen assays**

172 For the pathogen assays, we introduced an agar plug inoculated with hyphae of *Calonectria* sp. ( $P+$   
173 treatment), and an agar plug without the pathogen ( $P-$  control) to similarly aged/sized leaves within 10-  
174 14 days after endophyte inoculations (CITATION). Leaves with the  $P+$  or  $P-$  treatment were misted  
175 with sterile water two times a day (morning and afternoon) to maintain moisture. After four days, we

176 removed the plugs and took digital photos to analyze leaf area damage using ImageJ [v1.52r; Schneider  
177 et al. (2012)].

### 178 **3.2.5 Statistical Analyses**

179 We explored how leaf functional traits and foliar fungal symbionts correlated to herbivory and pathogen  
180 damage on leaves. We present the analyses at the leaf and at the plant level. Leaf functional traits were  
181 measured and are presented in their raw form, at the leaf level, while FEF data was explored and is  
182 presented at the plant level. In analyses where leaf functional traits and FEF are combined we used  
183 averages of the leaf functional traits.

184 To test for H2, we used a general linear mixed model (GLM) with XXXX as the response variable.  
185 To determine which fixed effects to include in the models we used the `vif` function in *R* to calculate  
186 the variance inflation factor for all explanatory variables (ACI, LT, LPS and LMA) (R Core Team,  
187 2023). We then created a correlation matrix with `cor` function to assess correlations among covariates.  
188 We opted to maintain explanatory variables pertaining to physical barriers (LT, LPS and LMA) and  
189 exclude ACI from subsequent linear models due to high collinearity with LPS (0.54) and LMA (0.73).  
190 Every variable kept exhibits some degree of collinearity and this is well recorded in the literature (CITE  
191 HERE).

192 Additionally, Principal Component Analysis (PCA) was used to reduce dimensions among covariates  
193 and reveal underlying interactions that could influence fungal endophyte abundance, diversity and com-  
194 munity composition in seedlings. The PCA was computed using the `prcomp` function in *R* statistical  
195 software (R Core Team, 2023). A complete PCA was computed with variables ACI, LT, LPS, and LMA

196 (FIGURE 2a?). We then proceeded to compute a PCA with the data from leaves of plants used in the  
197 ant ( $n = 210$ ) and pathogen assays ( $n = 192$ ).

198 The PCA revealed how covariates (LMA, ACI, Thickness and Toughness) interact. I overlapped tree  
199 species groups on the PCA axes to show how the variance in the data is explained by PC1 (60%) and  
200 PC2 (27%) (Fig. 4). This is indicative of correlation among covariates. Thickness and toughness were  
201 orthogonal to each other in PCA, indicative of low correlation.

## 202 **4 References**

203 Arnold, A. E., & Lutzoni, F. (2007). Diversity and host range of foliar fungal endophytes: Are tropical  
204 leaves biodiversity hotspots? *Ecology*, 88(3), 541–549. <https://doi.org/10.1890/05-1459>

205 Arnold, A. E., Mejía, L. C., Kyllo, D., Rojas, E. I., Maynard, Z., Robbins, N., & Herre, E. A. (2003).  
206 Fungal endophytes limit pathogen damage in a tropical tree. *Proceedings of the National Academy  
207 of Sciences*, 100(26), 15649–15654.

208 Bowman, E. A., & Arnold, A. E. (2021). Drivers and implications of distance decay differ for ectomy-  
209 corrhizal and foliar endophytic fungi across an anciently fragmented landscape. *The ISME Journal*,  
210 15(12), 3437–3454. <https://doi.org/10.1038/s41396-021-01006-9>

211 Callahan, B. J., McMurdie, P. J., Rosen, M. J., Han, A. W., Johnson, A. J. A., & Holmes, S. P. (2016).  
212 DADA2: High-resolution sample inference from Illumina amplicon data. *Nature Methods*, 13(7),  
213 581–583. <https://doi.org/10.1038/nmeth.3869>

214 Carbone, I., White, J. B., Miadlikowska, J., Arnold, A. E., Miller, M. A., Kauff, F., U'Ren, J. M., May,  
215 G., & Lutzoni, F. (2017). T-BAS: Tree-Based Alignment Selector toolkit for phylogenetic-based

placement, alignment downloads and metadata visualization: An example with the Pezizomycotina  
 tree of life. *Bioinformatics*, 33(8), 1160–1168. <https://doi.org/10.1093/bioinformatics/btw808>

Carbone, I., White, J. B., Miadlikowska, J., Arnold, A. E., Miller, M. A., Magain, N., U'Ren, J. M., &  
 Lutzoni, F. (2019). T-BAS Version 2.1: Tree-Based Alignment Selector Toolkit for Evolutionary  
 Placement of DNA Sequences and Viewing Alignments and Specimen Metadata on Curated and  
 Custom Trees. *Microbiology Resource Announcements*, 8(29), e00328–19. <https://doi.org/10.1128/MRA.00328-19>

Daru, B. H., Bowman, E. A., Pfister, D. H., & Arnold, A. E. (2019). A novel proof of concept for  
 capturing the diversity of endophytic fungi preserved in herbarium specimens. *Philosophical Transactions of the Royal Society B: Biological Sciences*, 374(1763), 20170395. <https://doi.org/10.1098/rstb.2017.0395>

Higgins, K. L., Arnold, A. E., Coley, P. D., & Kursar, T. A. (2014). Communities of fungal endophytes  
 in tropical forest grasses: Highly diverse host- and habitat generalists characterized by strong spatial  
 structure. *Fungal Ecology*, 8(1), 1–11. <https://doi.org/10.1016/j.funeco.2013.12.005>

McMurdie, P. J., & Holmes, S. (2013). Phyloseq: An R Package for Reproducible Interactive Analysis  
 and Graphics of Microbiome Census Data. *PLoS ONE*, 8(4), e61217. <https://doi.org/10.1371/journal.pone.0061217>

McMurdie, P. J., & Holmes, S. (2014). Waste Not, Want Not: Why Rarefying Microbiome Data Is  
 Inadmissible. *PLoS Computational Biology*, 10(4), e1003531. <https://doi.org/10.1371/journal.pcbi.1003531>

Oita, S., Ibáñez, A., Lutzoni, F., Miadlikowska, J., Geml, J., Lewis, L. A., Hom, E. F. Y., Carbone, I.,  
 U'Ren, J. M., & Arnold, A. E. (2021). Climate and seasonality drive the richness and composition

of tropical fungal endophytes at a landscape scale. *Communications Biology*, 4(1), 313. <https://doi.org/10.1038/s42003-021-01826-7>

R Core Team. (2023). *R: A Language and Environment for Statistical Computing* [Computer software]. R Foundation for Statistical Computing. <https://www.R-project.org/>

Rognes, T., Flouri, T., Nichols, B., Quince, C., & Mahé, F. (2016). VSEARCH: A versatile open source tool for metagenomics. *PeerJ*, 4, e2584. <https://doi.org/10.7717/peerj.2584>

Sarmiento, C., Zalamea, P. C., Dalling, J. W., Davis, A. S., Simon, S. M., U'Ren, J. M., & Arnold, A. E. (2017). Soilborne fungi have host affinity and host-specific effects on seed germination and survival in a lowland tropical forest. *Proceedings of the National Academy of Sciences of the United States of America*, 114(43), 11458–11463. <https://doi.org/10.1073/pnas.1706324114>

Schneider, C. A., Rasband, W. S., & Eliceiri, K. W. (2012). NIH Image to ImageJ: 25 years of image analysis. *Nature Methods*, 9(7), 671–675. <https://doi.org/10.1038/nmeth.2089>

Tellez, P. H., Arnold, A. E., Leo, A. B., Kitajima, K., & Van Bael, S. A. (2022). Traits along the leaf economics spectrum are associated with communities of foliar endophytic symbionts. *Frontiers in Microbiology*, 13, 927780. <https://doi.org/10.3389/fmicb.2022.927780>

Tellez, P. H., Rojas, E., & Van Bael, S. (2016). Red coloration in young tropical leaves associated with reduced fungal pathogen damage. *Biotropica*, 48(2), 150–153. <https://doi.org/10.1111/btp.12303>

U'Ren, J. M., & Arnold, A. E. (2017). 96 well DNA Extraction Protocol for Plant and Lichen Tissue Stored in CTAB. *Protocols.io*, 1–5.

U'Ren, J. M., Lutzoni, F., Miadlikowska, J., Zimmerman, N. B., Carbone, I., May, G., & Arnold, A. E. (2019). Host availability drives distributions of fungal endophytes in the imperilled boreal realm. *Nature Ecology & Evolution*, 3(10), 1430–1437. <https://doi.org/10.1038/s41559-019-0975-2>

260 Weiss, S., Xu, Z. Z., Peddada, S., Amir, A., Bittinger, K., Gonzalez, A., Lozupone, C., Zaneveld, J.  
261 R., Vázquez-Baeza, Y., Birmingham, A., Hyde, E. R., & Knight, R. (2017). Normalization and  
262 microbial differential abundance strategies depend upon data characteristics. *Microbiome*, 5(1), 27.  
263 <https://doi.org/10.1186/s40168-017-0237-y>

## 264 **5 Figures**

### 265 **5.1 Figure 1**

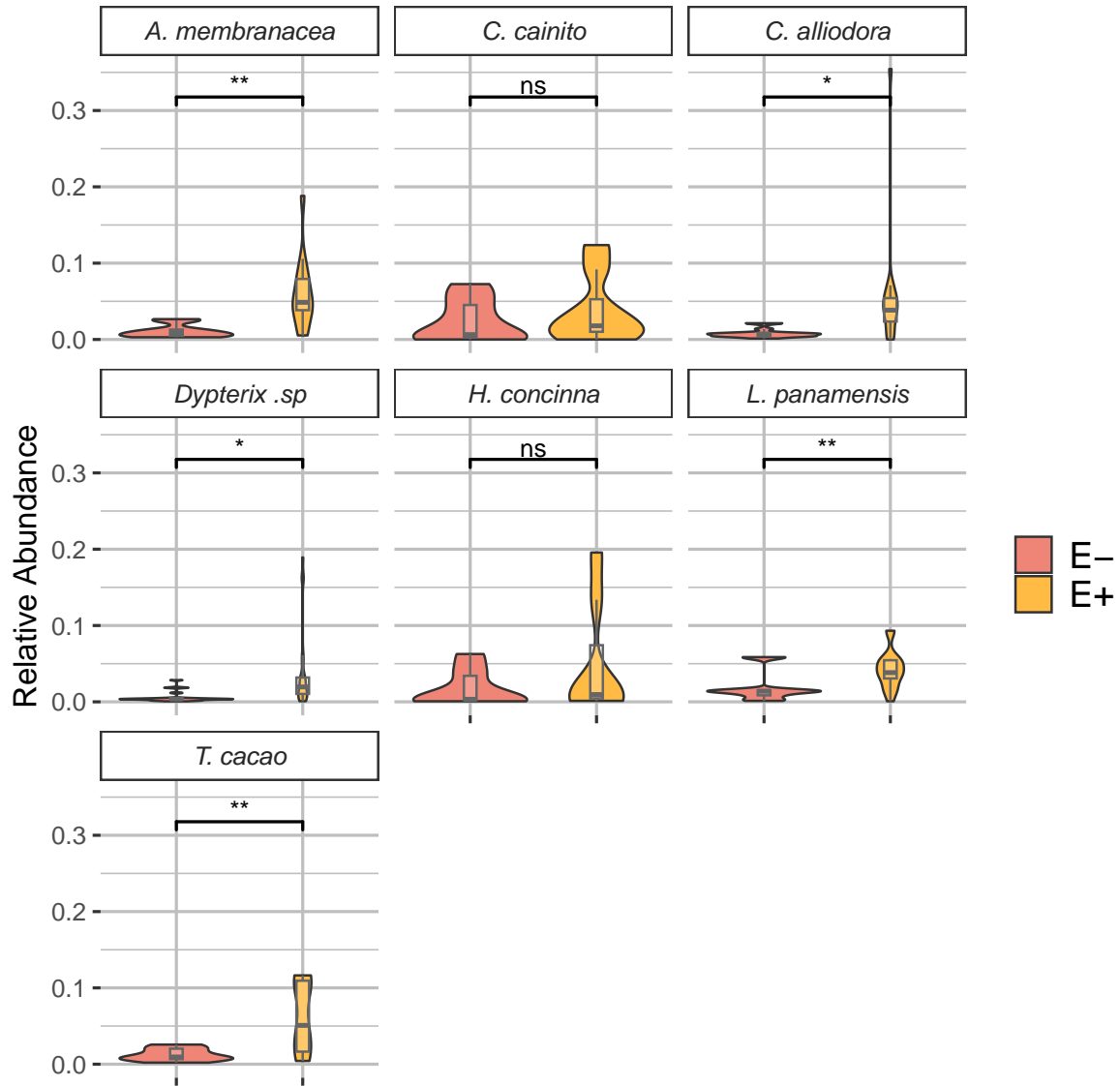


Figure 1: Relative abundance (RA) of Ascomycota OTUs of seven tree species used in the study. Violin plots show the distribution of the RA. The horizontal line within the embedded boxplots represents the median, the box represents the interquartile range (IQR), and the whiskers represent the 1.5xIQR. Outliers are represented by dots. Significant levels are represented by p = 0.05 (\*), p = 0.01 (\*\*), and p = 0.001 (\*\*\*).